Journal of Visualization, Vol. 10, No. 3 (2007)271-280

Regular Paper

Numerical Analyses of Flow around Airfoils Subjected to Flow Induced Vibration

Yokono, Y.* and Biswas, D.*

* Corporate Research & Development Center, Toshiba Corporation, 1 Komukai Toshiba-cho, Saiwai-ku, Kawasaki, 212-8582, Japan.

Received 8 December 2006
Revised 16 May 2007

Abstract : This paper describes extensive computer-based analytical studies on the details of unsteady flow behavior around airfoils subjected to flow induced vibration in turbo-machinery. To consider the time-dependent motions of airfoils, a complete Navier-Stokes solver incorporating a moving mesh based on an analytic solution of motion equation for airfoil translation and rotation was applied. The drag and lift coefficients for the cases of stationary airfoils and airfoils subjected to flow induced vibration were examined. From the numerical results in non-coupling case as out of consideration of the airfoil motion, it was found that the separation vortex consisted of large-scale rolls with axes in the span direction, and rib substructures with axes in the stream direction. In the coupling simulation including the airfoil motion, both the translation and the rotation displacement were gradually increased when the airfoil translation and rotation natural frequencies synchronize exactly with the oscillation frequency of the fluid force. In addition, the transformation from complex structure with rolls and ribs to two-dimensional aspect of only rolls could be visualized in three-dimensional simulation.

Keywords : Flow Induced Vibration, ALE, Flutter, Airfoil, Vortex.

1. Introduction

Demands for high efficiency and large capacity in a combined cycle generation plant are bringing long and thin blades in the compressor first cascade or the turbine final cascade. In these blades, the flow induced vibration might cause critical damage to the turbo-machinery. This flutter problem in turbo-machinery is one of the critical issues for improving its reliability, and a simulation method to predict the flutter phenomena is getting much more important. From this point of view, a great deal of experimental and numerical research has been done. Carstens (1995) presented unsteady pressure and lift coefficient for blade motions at different interblade phase angles. Eguchi and Wiedermann (1995) dealt with unstalled and stalled flutter using Navier-Stokes code with deforming mesh. Ekaterinaris and Platzer (1995) applied two-dimensional Navier-Stokes code to a blade stall flutter problem. Aso and Kumamoto (1995) visualized flow fields of oscillating airfoil by experimental and computational studies. Alam et al. (2007) developed a two-dimensional direct numerical simulation (DNS) scheme to calculate the flow around an oscillating cylinder. Fujisawa et al. (2005) indicated that the large-scale structure of vortex shedding was almost removed by the rotational oscillation of the cylinder. Suzuki and Arakawa (2006) analyzed the mechanism of high attack anglel three-dimensional flows around the turbine with the flow visualization and the numerical analysis, focusing on the off-design condition. Shao et al. (2007) showed that vortex shedding from both sides of the cylinder could be effectively suppressed and discussed the mechanism of the suppression.

In order to clarify the interaction between airfoil structure and the flow induced force, numerical simulation must deal with large separation regions and the exact time history of the drag and lift coefficients should be determined. Although two-dimensional analyses have been performed for the flutter problem accompanying a separation vortex, it has been considered to be difficult to obtain the true separation vortex in such analyses because the vortex structure is essentially three-dimensional. Therefore, in the present study, a comparison is made between the two- and three-dimensional analyses for NACA0012 airfoils subjected to stationary and flow induced vibration. To consider the time-dependent motions of airfoils, a complete Navier-Stokes solver incorporating a moving mesh based on an analytic solution of motion equation for airfoil translation and rotation is applied. Based on the obtained flow induced force upon the airfoil and the flow visualization, the separation vortex structure is examined in detail.

2. Nomenclature

C = damping coefficient
CD = drag coefficient
CL = lift coefficient
D = chord length
f = natural frequency
F = force
K = resistance
M = mass
MO = moment
P = pressure
Re = Reynolds number
v = velocity
θ = rotation angle
γ = damping factor
ω = natural circular frequency
λ = logarithm damping rate
ρ = density

Subscripts
n: translation
r: rotation

3. Computational Model

The governing equations in the present analysis are given below as dimensionless form;

Continuity equation

$$\nabla \cdot v = 0 \tag{1}$$

Momentum equation

$$\frac{Dv}{Dt} = -\nabla p + \frac{1}{\mathrm{Re}} \nabla^2 v \tag{2}$$

The solution of these equations is obtained numerically with a finite difference method.. A third-order upwind difference implicit scheme developed by Kawamura et al. (1984 and 1985) is used. The number of consecutive grid points in the scheme adopted here is five. This scheme introduces numerical damping for the convection terms. The mechanism used in LES model to dissipate energy from resolved to sub-grid scales is included implicitly in the numerical scheme itself (Yokono, 1997; Biswas and Iwasaki, 2002). This type of models is also called implicit LES (Rizzetta et al., 2005; Morgan et al., 2005). Some interesting results regarding the advantage and performance of this implicit LES scheme in the case of bluff-body flows is presented by Tamura et al. (1990).

To consider the time-dependent motions of airfoils, arbitrary Lagrangian-Eulerian formulation was employed. A complete Navier-Stokes solver incorporating a moving mesh was applied. At each time step, the boundary grid points were given by an analytic solution of motion equations for a rigid airfoil and the inner grid points were generated by solving the Poisson equation according to the Steger and Sorenson method (Steger, 1979). The numerical model of airfoil motion is shown in Fig. 1 and the motion equation of airfoil translation and rotation are given bellow. Here, the motion equation deals with viscous damping. Since the main aim of this work is to study the flow induced vibration characteristics, the vibration parameters for the airfoil is selected to correspond with the fluctuation frequency of the fluid force.

At the design stage, the flow conditions should cover a wide range of Reynolds number other than the operating load condition. Also, assuming the trouble or from the viewpoint of the risk management, an examination in special condition may be needed. The goal of our work is to develop a reliable engineering tool to be used in the design and development of power generating turbine

device. The numerical model used in the engineering tool for designing should have the capability of reliably predicting the turbulent flow characteristics including laminar to turbulent transitional phenomena. Therefore, the attack angle of inlet velocity was 15 degrees and the Reynolds number normalized by the chord length and free stream velocity was 1.0×10^4, where the laminar to turbulent transitional phenomena play a dominant role. Analyses of both non-coupling case as out of consideration of the airfoil motion and coupling case as varying these motion equation parameters were conducted.

The computational domain in the present study is shown in Fig. 2. The NACA0012 airfoil having a unit chord length was placed in a C-shape grid system. The all direction fluid traction was assumed free at the outlet, which is placed downstream at 10 times the chord length. On the airfoil surface, non-slip condition was specified. A cyclic condition was employed on a span direction boundary. In two-dimensional simulations, 323 x 61 grid points were deployed. In three-dimensional calculations, adding the case of two-dimensional analysis, 40 grid points were deployed in the airfoil span direction. The calculation parameters are summarized in Table 1.

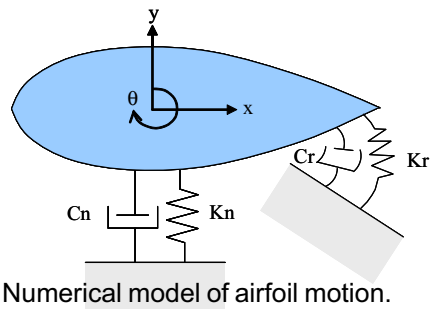

Fig. 1. Numerical model of airfoil motion.

Translation motion equation

$$M_n y'' + C_n y' + K_n y = F_n \tag{3}$$

Rotation motion equation

$$M_r \theta'' + C_r \theta' + K_r \theta = F_r \tag{4}$$

Here,

$$f_n = \frac{\omega_n}{2\pi} \quad \omega_n = \sqrt{\frac{K_n}{M_n}} \quad \gamma_n = \frac{C_n}{2M_n} \quad \lambda_n = \frac{\gamma_n}{f_n}$$

$$f_r = \frac{\omega_r}{2\pi} \quad \omega_r = \sqrt{\frac{K_r}{M_r}} \quad \gamma_r = \frac{C_r}{2M_r} \quad \lambda_r = \frac{\gamma_r}{f_r}$$

Table 1 Calculation Parameter.

Airfoil Shape	NACA0012
Reynolds Number	1.0×10^4
Attack Angle	15 degrees
Span Length	same as chord length
Grid Number	323x61 (2D) 323x61x40 (3D)
Calculation time step	0.005

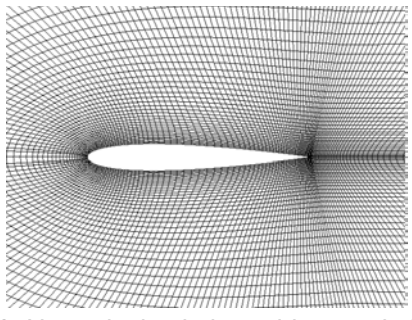

Fig. 2. Numerical solution grid around airfoil.

4. Result and Discussion

4.1 Flow around Airfoil in the Case of Non-Coupling

The flow visualizations around a NACA0012 airfoil are shown in Fig. 3. These figures show the instantaneous pressure distribution for the case of non-coupling for two- and three-dimensional simulation results. The color bar represents the calculated non-dimensional pressure value. The color scale in the fringe figure of two-dimensional results is selected to indicate min and max pressure value. In the two-dimensional simulation as shown in Fig. 3(a), a number of vortices emerged on the suction surface, separated from the surface, and became large-scale vortices. As these vortices were shed into the wake, near the trailing edge, large-scale vortices generated and flowed downstream.

Figure 3(b) shows pressure isosurfaces in the three-dimensional simulation. The isosurface figure of three-dimensional results represents three curvilinear surfaces equivalent to the pressure value of -0.37, -0.26 and -0.07, respectively. The color is selected to distinguish these three surfaces. It is not possible to have one-to-one correspondence between the pressure iso-surface and the vortex structure. The purpose of this work is not to perform a detail study on the unsteady vortex structural behavior. In order to have some overall understanding of unsteady flow characteristics in 3-dimensional flow, the pressure iso-surface is adopted. Large scale vortices with axes in the span direction and longitudinal vortices with axes in the stream direction, which are called rolls and ribs, respectively (Bernal, 1986; Brown, 1974), were observed. Span directional rolls were transformed by the ribs, and a complicated three-dimensional vortex structure appeared. The mechanism responsible for generating these rolls and ribs was thought to be as follows (Hussain, 1986; Metcalfe, 1987). The flow separated near the trailing edge, generating two-dimensional large-scale roll with axes in the span direction. These two opposite rolls interfered with each other, longitudinal ribs were formed, and the rolls were contorted in the span direction by the ribs. Therefore, it has been considered to be difficult to obtain the true separation vortex in two-dimensional simulation because the vortex structure should be essentially three dimensional.

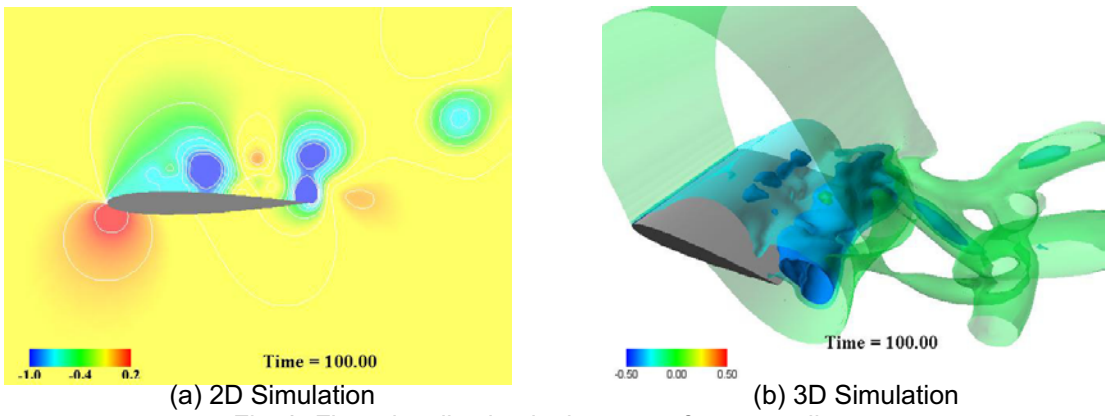

(a) 2D Simulation (b) 3D Simulation

Fig. 3. Flow visualization in the case of non-coupling.

4.2 Drag and Lift Coefficients in the Case of Non-Coupling

Figure 4 shows the time history of a drag and a lift coefficient in the case of non-coupling. In the two-dimensional analysis, both drag and lift coefficients showed regular periodical fluctuation. For the three-dimensional calculation, the lift coefficient showed the time history coupled the same frequency as that of two-dimensional analysis with much lower frequency. Although the time-averaged drag coefficient showed almost the same value in the two- and three-dimensional analyses, the time averaged lift coefficient in the three-dimensional analysis was smaller than that in the two-dimensional analysis.

The power spectrums of lift coefficient in the case of non-coupling are shown in Fig. 5. In the two-dimensional simulation as shown in Fig. 5(a), the power spectrum for lift coefficient had a sharp peak at frequency 0.64 with another peak at integral multiplication of the peak frequency. The peak frequency for three-dimensional analysis was 0.68, which was higher than that of the

two-dimensional analysis. No clear peaks at integral multiplication of the peak frequency were observed. A broad band spectrum appeared in comparison with the two-dimensional result. Therefore, it was found that both the fluid force magnitude and frequency upon the airfoil were different between two- and three-dimensional analyses.

Experimental lift coefficients and its dependency on flow attack angle are compared with the present results. NACA report(Jacobs and Sherman,1939) presented a lift coefficient of 0.8 and Sandia report(Sheldahl and Klimas,1981) presented a lift coefficient of 0.3 under the same Reynolds number conditions in this lower range for attack angle of 15 degree. Results on lift coefficient for lower Reynolds number range, where not much change in lift coefficient with the Reynolds number is observed, are somewhat different in these two reports. The predicted value of lift coefficient in 3D computation is 0.65 and 2D prediction of lift coefficient is 1.1. Even allowing for the discrepancies in measured lift coefficient, the 3D result is closer to the experimental data as compared to the 2D simulation.

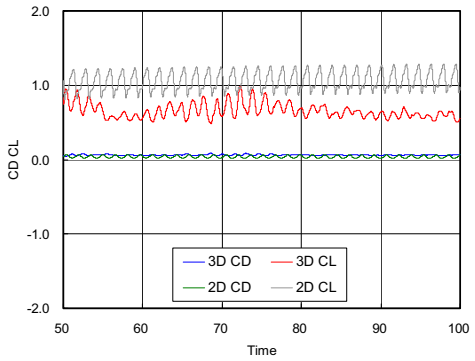

Fig. 4. Drag and lift coefficient in the case of non-coupling.

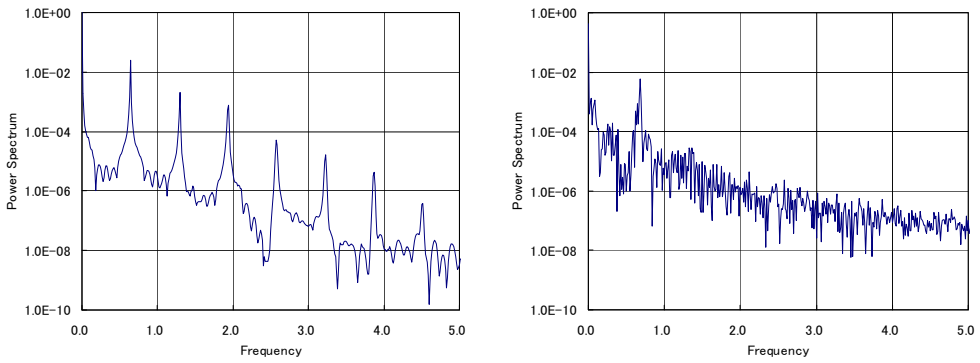

(a) Two-dimensional simulation (b) Three-dimensional simulation

Fig. 5. Power spectrum of lift coefficient in the case of non-coupling.

4.3 Flow around Airfoil in the Case of Coupling

Figure 6 shows the pressure distribution around the airfoil subjected to flow induced vibration. In flow induced vibration analysis, calculations were restarted with the non-coupling result at the non-dimensional time of 100 as the initial condition. Figure 6(a) indicates two-dimensional simulation result in the case that both the airfoil translation and rotation natural frequency synchronize exactly with the oscillation frequency of the fluid force with no damping, such as fn = 0.64, fr = 0.64 and $2\gamma = 0$. Large-scale separation vortices generate and flow downstream on the suction surface, is similar to the case of non-coupling. The animation of these results showed the periodic translation and rotation motion of the airfoil in accord with fluid force fluctuation based on the generation of these vortices. Figure 6(b) shows the pressure isosurface of the three-dimensional simulation result at fn = 0.68, fr = 0.68 and $2\gamma = 0$. From this figure, at the time = 150 when the flow was fully developed, it was found that the rib structure diminished and the vortex structure became two-dimensional. The animation of this case clearly showed the transformation from the complex structure with large scale vortices with axes in the span direction and longitudinal vortices with axes in the stream direction, which are called rolls and ribs, to the two-dimensional aspect of only rolls.

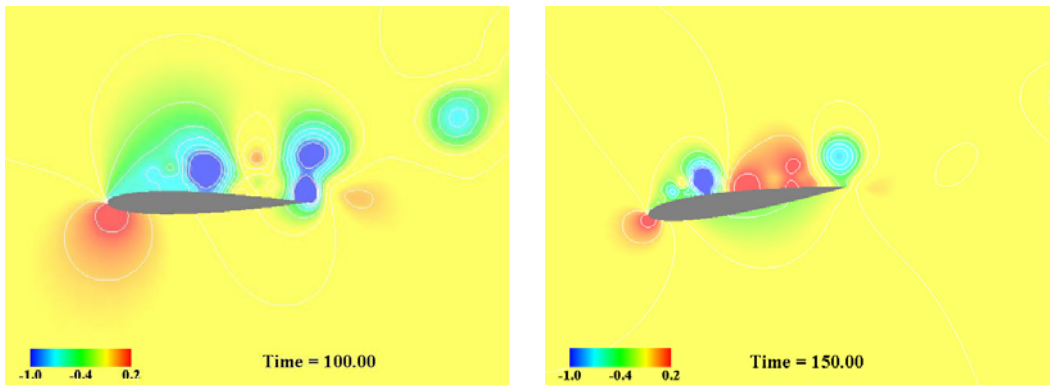

(a) 2D Simulation (*fn* = 0.64 *fr* = 0.64 2γ= 0)

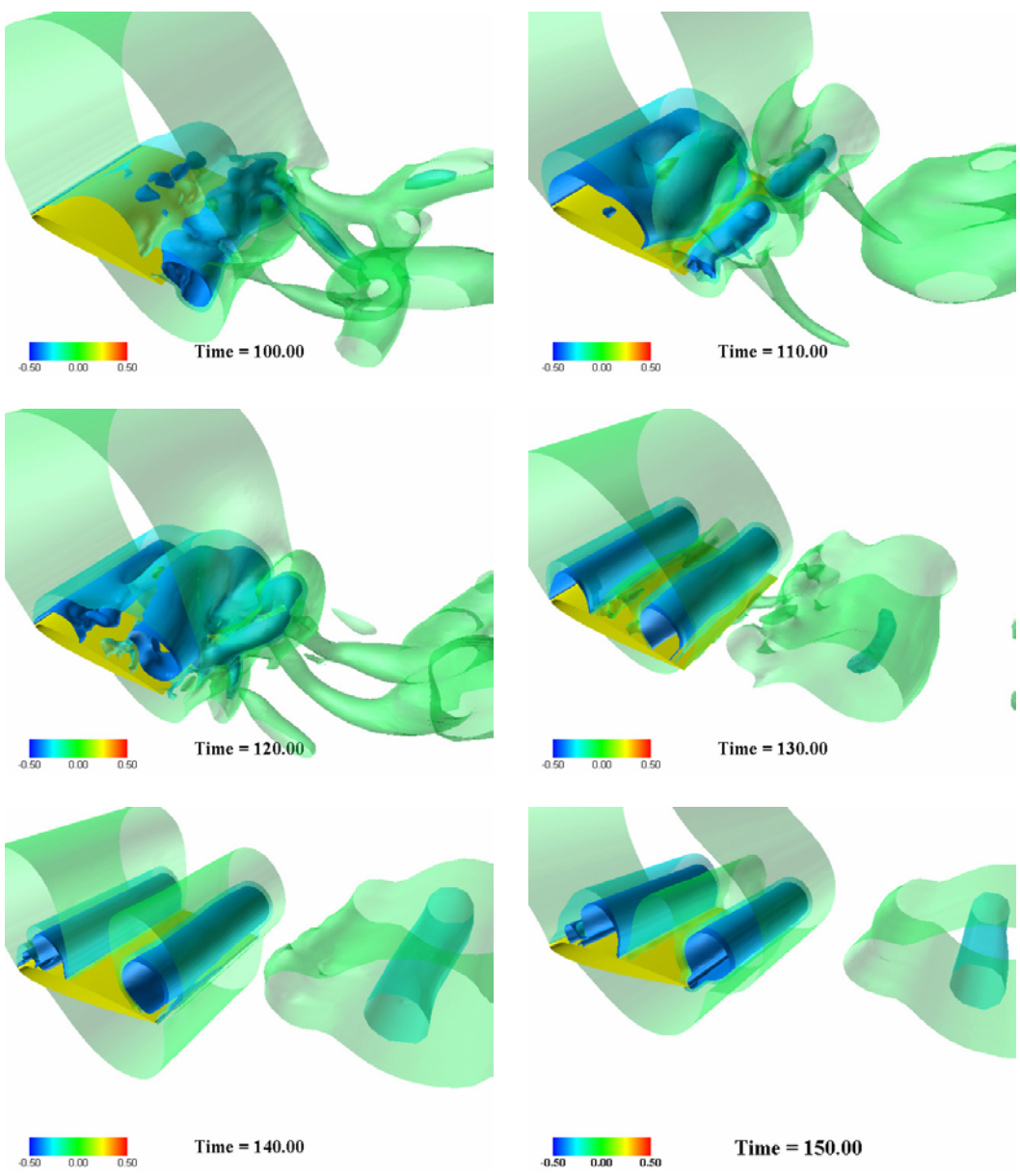

(b) 3D Simulation (*fn* = 0.68 *fr* = 0.68 2γ= 0)

Fig. 6. Flow visualization in the case of coupling.

In the case of stationary airfoil, vortex is formed as Karman vortex and transforms to two-dimensional large scale vortex having its axis aligned towards the span-wise direction of blade. This transformation phenomenon is called vortex rolling. In this transformation process, the modulus of vorticity vector is high enough so that a local rollup of the surrounding fluid is possible. They keep their shape approximately during a time long enough in front of the local turnover time. Under such conditions, the cores of the vortices should be pressure lows. Indeed fluid parcel winding around the vortex will be (in a frame moving with the parcel) in approximate balance between centrifugal and pressure gradient effects. Here, the force acts from the saddle points between the vortices formed during two consecutive times towards the direction of stretching of vortex and a vortex structure called rib is formed. This rib formation leads to a transformation in shape of the rolling vortex (or leads to the vortex break down process). Therefore, as shown in figure, the vortex structure around stationary airfoil is very complex and three-dimensional in nature. On the other hand, in the case of airfoil vibrating at some typical frequency, which corresponds to the frequency of vortex generation on the airfoil itself, phase angle of roll vortex along the span-wise get coincided due to the blade vibration and it is difficult to occur interaction between rolling vortices formed during two successive times. Therefore the vortex structure under such conditions is expected to two-dimensional in nature.

4.4 Fluid Forces and Displacement of Airfoil in the Case of Coupling

Figure 7 shows the time history of the fluid forces and the airfoil displacements for two-dimensional simulation result at both the airfoil translation and rotation natural frequency of 0.64. The drag, lift and moment coefficient as shown in Fig. 7(a) exhibited relatively more volatility than in the case of non-coupling. The magnitude of fluctuation varied in time and was much greater than in the case of non-coupling. Figure 7(b) shows the airfoil translation and rotation displacement. Both translation and rotation displacement fluctuated periodically. The amplitude of translation displacement had a somewhat lower frequency than the airfoil motion frequency and was gradually increased. Figure 8 shows the case of three-dimensional simulation results when the airfoil translation and rotation natural frequency synchronize exactly with the oscillation frequency of the fluid force. The lift and moment coefficients as shown Fig. 8(a) were gradually increased from the region of t = 120, as shown Fig. 8(a). This means that the flow was not fully developed until around t = 120, as the coupling simulation was restarted with the non-coupling result at time of t = 100. The translation and rotation displacement shown in Fig. 8(b) had the time history coupled at the same frequency as the airfoil motion with much lower frequency and the magnitude of fluctuation gradually increased.

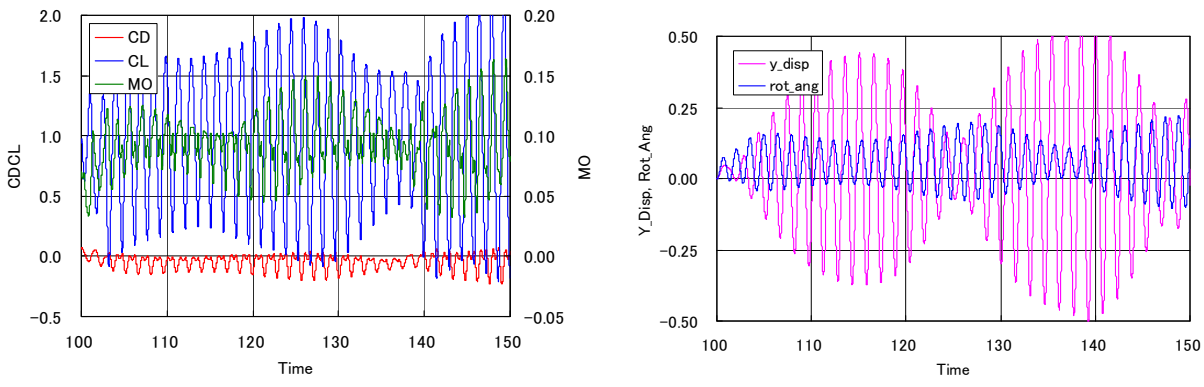

(a) Drag, lift and moment (b) Translation and rotation displacement

Fig. 7. 2D Simulation in the case of coupling (fn = 0.64 fr = 0.64 2γ= 0).

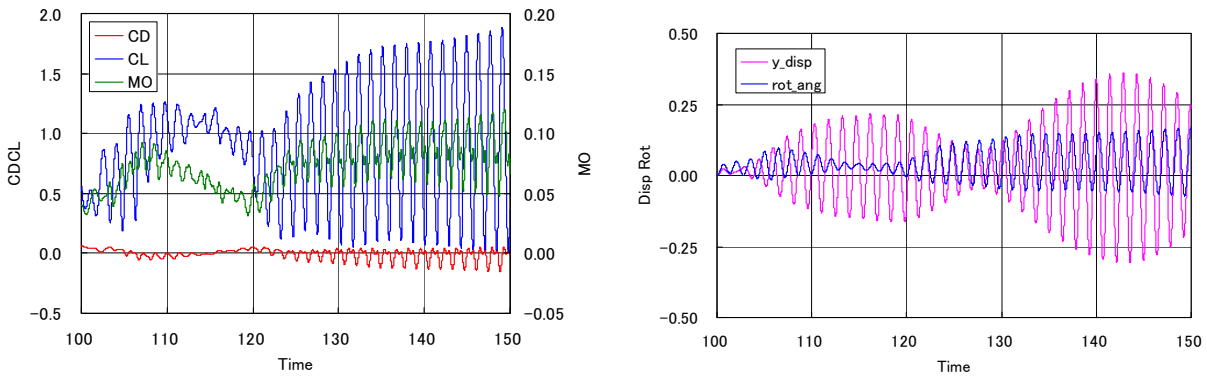

(a) Drag, lift and moment (b) Translation and rotation displacement

Fig. 8. 3D Simulation in the case of coupling (*fn* = 0.68 *fr* = 0.68 2γ= 0).

4.5 Pressure Cross Correlation

The cross correlation between the time history and the span direction distribution of the pressure fluctuation is defined as follows;

$$R(z,\tau) = \frac{\overline{p'(z_0,t)p'(z,t+\tau)}}{\sqrt{\overline{p'(z_0,t)^2}}\sqrt{\overline{p'(z,t)^2}}} \tag{5}$$

Here, z is the span length and $\tau$is the time lag.

The cross correlation in case of the non-coupling 3D simulation is shown Fig. 9(a). The measuring point of pressure fluctuation was the 0.9 chord length downstream from the leading edge of the airfoil. The time averaging was accomplished with the 2000 time steps from t = 80 to t = 100. The cross correlation indicated a weak periodicity in time according to the large scale role structure with axes in the span direction and varied along the span direction due to the longitudinal rib with axes in the stream direction. Considering with the visualization of pressure isosurface, it was clearly understood that the separation vortices had a complex three-dimensional structure. Figure 9(b) shows the cross correlation in the case of coupling 3D simulation. The measuring point was the same as in the non-coupling case. The time averaging was carried out from t = 130 to t = 150, in which range the flow was regarded as being fully developed. Absolutely regular periodicity of the correlation in time was observed. There were no variations along the span direction. Therefore, it was found that the structure of the vortices consisted of two-dimensional rolls only in the fully developed flow around the airfoil subjected to flow induced vibration.

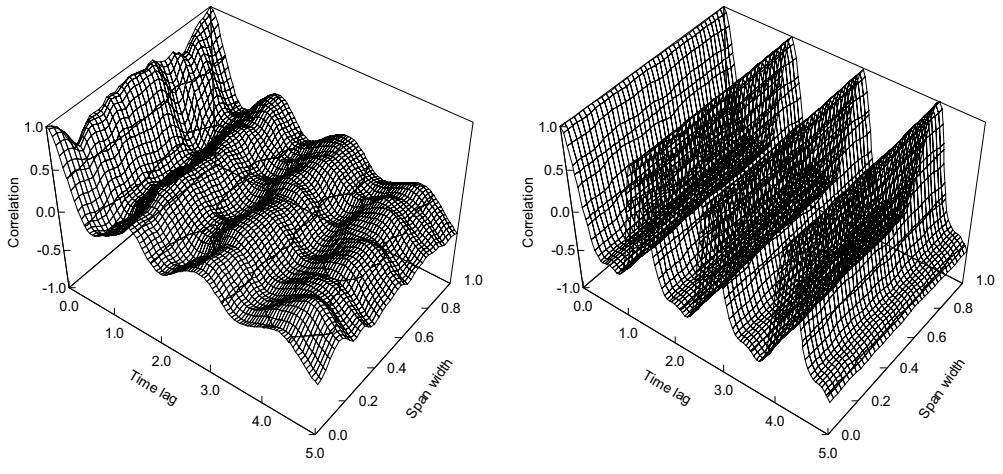

(a) Non-coupling (*fn* = ∞ *fr* = ∞ 2γ= 0) (b) Coupling (*fn* = 0.68 *fr* = 0.68 2γ= 0)

Fig. 9. Pressure cross correlation (x = 0.9) of 3D simulation.

5. Conclusion

In order to predict the flutter phenomena, a complete Navier-Stokes solver incorporating a moving mesh based on the analytical solution of the airfoil motion equation was applied. The two- and three-dimensional analyses were compared in the cases of non-coupling / coupling between the airfoil structure motion and the fluid forces fluctuation.

Three-dimensional analysis for the non-coupling indicated that the airfoil surface pressure distribution varied in the span direction. By visualizing pressure distributions, it was found that the separation vortex consisted of large-scale rolls with axes in the span direction and rib substructures with axes in the stream direction. The time averaged lift coefficient in the three-dimensional analysis was smaller than that in the two-dimensional analysis. The peak frequency of the power spectrum for both drag and lift coefficients was higher in the three-dimensional analysis. In the coupling case such that the airfoil translation and rotation natural frequency synchronize exactly with the oscillation frequency of the fluid force, the airfoil translation and rotation displacement had the time history coupled at the same frequency as the airfoil motion with much lower frequency and the magnitude of fluctuation gradually increased. The three-dimensional analysis could simulate the transformation from the complex three-dimensional structure with rolls and ribs to the two-dimensional aspect of rolls only in the fully developed flow around the airfoil subjected to flow induced vibration.

References

Alam, M. M., Fu, S. and Zhou, Y., Generation of Vortices by a Streamwise Oscillating Cylinder, Journal of Visualization, 10-1 (2007), 65-74.

Aso S. and Kumamoto Y., Experimental and computational studies on separated flows around oscillating airfoil, Unsteady Aerodynamics and Aeroelasticity of Turbomachines, (1995), 321-331.

Bernal, L. P. and Roshko, A., Streamwise vortex structure in plane mixing layers, Journal Fluid Mechanics, 170 (1986), 775-816.

Biswas, D. and Iwasaki H., Application of a Two-equation Low-Reynolds Number Version Turbulent Model to Transitional Flows, AIAA Paper, 2002-2748 (2002).

Brown, G. L. and Roshko, A., On density effects and large structures in turbulent mixing layers, Journal Fluid Mechanics, 64 (1974), 775-816.

Carstens V., Computation of unsteady transonic 3d flow in oscillating turbomachinery bladings by an Euler algorithm with deforming grids, Unsteady Aerodynamics and Aeroelasticity of Turbomachines, (1995), 73-91.

Eguchi T. and Wiedermann A., Numerical Analysis of Unstalled Flutter Using a Navier-Stokes Code with Deforming Meshes, Unsteady Aerodynamics and Aeroelasticity of Turbomachines, (1995), 237-253.

Ekaterinaris J. A. and Platzer M. F., Progress in the analysis of blade stall flutter, Unsteady Aerodynamics and Aeroelasticity of Turbomachines, (1995), 287-302.

Fujisawa, N., Ugata, M. and Suzuki, T., A study on drag reduction of a rotationally oscillating circular cylinder at low Reynolds number, Journal of Visualization, 8-1 (2005), 41-48.

Hussain, A.K.M.F., Coherent Structures and Turbulence, Journal Fluid Mechanics, 173 (1986), 303-356.

Jacobs, E. N. and Sherman, A., Airfoil section characteristics as affected by variations of the Reynolds number, NACA Report, 586 (1939).

Kawamura, T., Kuwahara, K. and Takami, H., Computation of High Reynolds Number Flow Around a Circular Cylinder with Surface Roughness, AIAA Paper, 1984-0340, (1984).

Kawamura, T., and Kuwahara, K., Direct Simulation of a Turbulent Inner Flow by Finite-Difference Method, AIAA Paper, 1985-0376 (1985).

Metcalfe, R. W., Orszag, S. A., Brachet, M. E., Menon, S. and Riley, J. J., Secondary instability of a temporally growing mixing layer, Journal Fluid Mechanics, 184 (1987), 207-243.

Morgan, P. E., Rizzetta, D. P. and Visbal, M. R., Large-Eddy Simulation of Separation Control for Flow Over a Wall-Mounted Hump, AIAA Paper, 2005-5017 (2005).

Rizzetta, D. P., and Visbal. M. R., Numerical Study of Active Flow Control for a Transitional Highly-Loaded Low-Pressure Turbine, AIAA Paper, 2005-5020, (2005).

Shao, C. P., Wang, J. M. and Wei, Q. D., Visualization Study on Suppression of Vortex Shedding from a Cylinder, Journal of Visualization, 10-1 (2007), 57-64.

Sheldahl, R. E.and Klimas, P. C., Aerodynamic Characteristics of Seven Symmetrical Airfoil Sections through 180-Degree Angle of Attack for Use in Aerodynamic Analysis of Vertical Axis Wind Turbines, Sandia National Laboratories energy report, (1981).

Steger, J. L. and Sorenson, R. L., Automatic mesh-point clustering near a boundary in grid generation with elliptic partial differential equations, Journal of Computational Physics, 33 (1979), 405-410.

Suzuki, M. and Arakawa, C., Flow on Blades of Wells Turbine for Wave Power Generation, Journal of Visualization, 9-1 (2006), 83-90.

Tamura, T., Ohta, I. and Kuwahara, K., On the Reliability of Two-Dimensional Simulation for Unsteady Flows around a Cylinder-Type Structure, Journal Wind Engineering and Industrial Aerodynamics, 35 (1990), 275-298.

Yokono, Y., Two- and Three-Dimensional Analyses of Flow Around Airfoils Subjected to Forced Oscillation, ASME AD-53-3, Fluid-Structure Interaction, Aeroelasticity, Flow-Induced Vibration and Noise, 3 (1997), 197-204.

Author Profile

Yasuyuki Yokono: He received his M.Sc .(Eng) and Ph D. in Mechanical Engineering in 1982 and 1985, respectively from Sophia University. He has been working at Toshiba Corporation from 1985. During 1992-1994, he worked at Tokyo Institute Technology as a visiting associate professor. His recent research interests are computational fluid dynamics, computer graphics, thermal designs of electronic equipment and thermal-hydrodynamics in power plant.

Debasish Biswas: He received the M.Tech degree in mechanical engineering from the Indian Institute of Technology, Delhi, India in 1984, and the Dr.Eng. in energy science from the Tokyo Institute of Technology, Tokyo, Japan, in 1987. In 1988, he joined the Toshiba Research and Development Center, Japan, (presently senior research engineer) and has since been working on the design and development of heavy electrical appliances. His field of research is the modeling of unsteady laminar to turbulent transitional flow, reactive flow (combustion, plasma phenomena), unsteady transitional heat transfer problem, flow-induced noise and vibration problem, etc.